HEAT TRANSFER NUMERICAL MODELING DURING JOMINY END-QUENCH TEST OF THE SAE 1045

Augusto César de Brito Geroldo, augustogeroldo@yahoo.com.br *
César Rolando Nunura Nunura, nunura_cesar@yahoo.es *
PUCRS – Pontifical Catholic University of Rio Grande do Sul, Av. Ipiranga, 6681, Partenon, ZipCode: 90.619-900, Porto Alegre, R.S., Brazil.
Wilson Hormaza, whormaza@uniandes.edu.co **
UNIANDES – Universidad de Los Andes, Cra 1 Este No. 19A-40. Bogotá, Colômbia.
Jaime Álvares Spim, spim@ct.ufrgs.br ***
UFRGS – Federal University of Rio Grande do Sul, Av. Bento Gonçalves, 9500, Agronomia, Zip Code: 91.500-970, Porto Alegre, R.S., Brazil
Carlos Alexandre dos Santos, carlos.santos@pucrs.br *
PUCRS – Pontifical Catholic University of Rio Grande do Sul, Av. Ipiranga, 6681, Partenon, Zip Code: 90.619-900, Porto Alegre, R.S., Brazil.

Abstract: The Jominy test, also called End-Quench Test, is the most commonly experimental method used to characterize the hardenability of the steels. During the test the cooling rate, which is maximum in the end-face and decreases progressively from the quenched end along the length of the bar, alters the resultant microstructure. For this test a round bar specimen that is 100 mm (4 inch) in length and 25 mm (1 inch) in diameter is heat to the austenitizing temperature of the steel with a holding time of 30 minutes. After that, one end-face of the specimen is quenched by spraying it with a jet of water. So, it is important to achieve full hardness to a certain minimum deep after cooling. Mathematical modeling is frequently used to prediction the hardenability of the steels, but these models are unclear and locked. The objective of this work is the development of a heat transfer numerical model based on the finite difference technique coupled with a phase transformation algorithm applied to Jominy test. This model has been used to provide the theoretical results concerning the rate of cooling at different distances from the quenched end. Experiments were performed with SAE 1045 steel, varying austenitizing temperatures (850°C, 900°C, 950°C). After cooling, two diametrically opposite flats (0.38 mm - 0.015 inch) deep and parallel to the axis of the bar were ground and the hardness was measured along the flats. The experimental hardness profiles were compared with theoretical predictions furnished by the developed numerical model.

Key-words: SAE 1045 steel, Jominy test, Heat transfer, Hardness, Numerical Modeling.

1. INTRODUCTION

The hardenability is the relative ability of steel to be deep-hardened which depends on cooling rates. The hardenability is unique to a given steel composition, austenitization condition, grain size and previous microstructure. The method which has been adopted almost universally is the Jominy end-quench test. The ASTM A 225 provides all information about the test, including the specimen (Figure 1), the device (Figure 2) and the operational procedures.

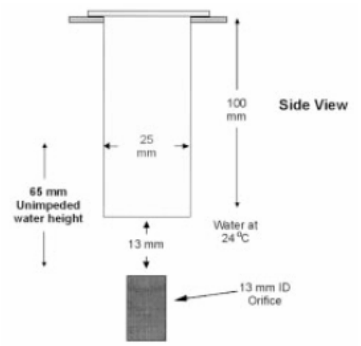

Figure 1. Specimen for the Jominy test [ASTM A 225].

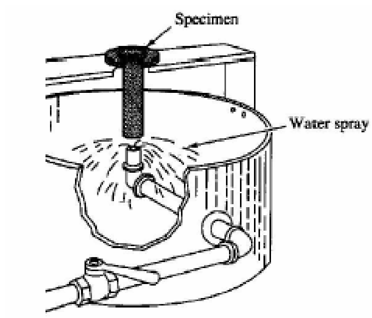

Figure 2. Schematic representation of the device used in the Jominy test [Chiaverinni, 2005].

As the initial microstructure has a high influence on the hardenability, the specimen is normalized before the test. In the test a cylindrical steel bar is heated up to its austenitic state and then it is out in a fixation and quenched by spraying water on its lower end. The hardness is measured at increasing distance from the quenched end (1/16 inch until 1 inch and 1/8 inch until 2 inch), as shown in Figure 3. The curve representing the hardness variation in function of distance from the quenched end of the specimen is called the Jominy hardenability curve.

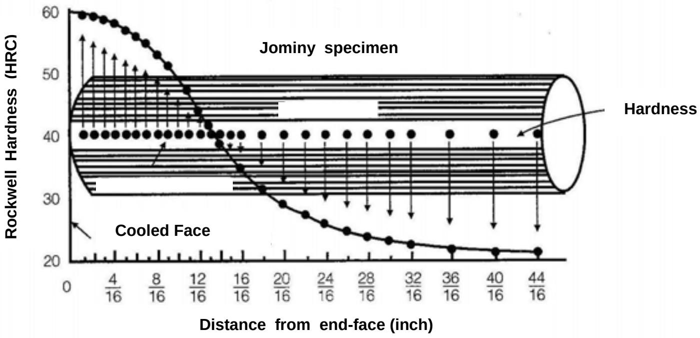

Figure 3. Representation of the plotted hardenability curve [Costa e Silva, 2006].

The inflection point in the hardenability Jominy curve often corresponds to 50% martensite, although the hardness of the martensite depends on carbon content. The evolution of the transitions phase is usually described in time-temperature transformation diagram (isothermal-transformation or continuous-cooling-transformation), as shown in Figure 4.

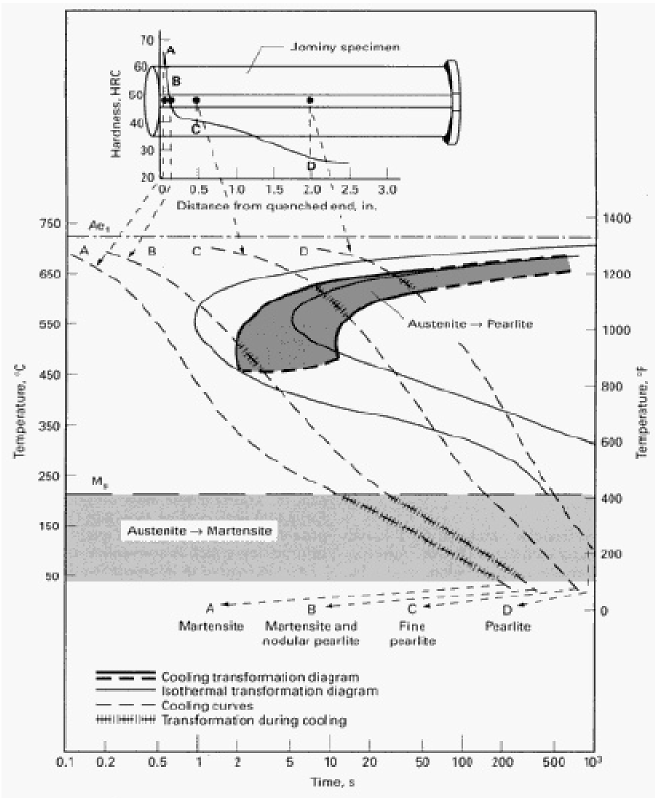

Figure 4. Correlation between continuous-cooling-transformation diagram and microstructure formation during the Jominy test [ASM Handbook v. 4].

There are a lot of works upon estimations of Jominy end-quench test, e.g. [Homberg, 1996; Masson, 2002; Song, 2007]. Homberg presented a model for the diffusive austenite-pearlite coupled with the non-diffusive austenite-martensite phase transformation, comparing our results with results presented by literature. Masson et. al. developed a numerical method for the two-dimensional estimation of a convection heat transfer coefficient for the Jominy test by solving a nonlinear inverse heat conduction problem. Based on a previous work, Song and others analyzed the Bai-hai's nonlinear equation method for predicting the Jominy end-quenched curves of multi-alloying carbon steel and with single-alloying element medium carbon steel. The curves predicted by the improved model agreed with the experimental results very well. Cobos, Reyes and Garcia used a finite elements model carried out in CosmosWorks version 2006 to analyze the cooling rate and fall of temperatures in different positions of the test specimen. The simulated results were located in a diagram of isothermic transformation comparing the results with the validation of the Jominy test and the different obtained hardness. The objective of this work is the development of a heat transfer numerical model based on the finite difference technique coupled with a phase transformation algorithm applied to Jominy test.

2. THE MATHEMATICAL MODEL

In the Jominy test, heat flow through the specimen can be reasonably approximated as a one-dimensional heat transfer problem, can be analyzed by [Spim, 1996]:

$$\rho c \frac{\partial T}{\partial t} = k \frac{\partial^2 T}{\partial x^2} + \dot{q} \tag{1}$$

where ρ, c, k are respectively density [kg/m^3], specific heat [J/kg.K] and thermal conductivity [W/m.K], T is temperature, t is time [s] and x is distance along the x-axis [m]. The term $\dot{q}$ on the right hand side of Eq. (1) is a heat source term which is incorporated to account for the latent heat of transformation, and is given by:

$$\dot{q} = \rho L \frac{\partial f_S}{\partial t} \tag{2}$$

where L is the latent heat of transformation [J/kg] and f_S is the phase transformation fraction. When treating the non-phase transformation heat flow, the governing equation is similar to Eq. (1) expect that the $\dot{q}$ term is not included.

Eq. (2) can be related to temperature as follows:

$$\frac{\partial f_S}{\partial t} = \frac{\partial f_S}{\partial T} \frac{\partial T}{\partial t} \tag{3}$$

Substitution of Eqs. (2) and (3) into Eq. (1), gives:

$$\rho\left(c - L.\frac{\partial f_S}{\partial T} \right)\frac{\partial T}{\partial t} = k\left(\frac{\partial^2 T}{\partial x^2}\right) \tag{4}$$

The term (L. $\frac{\partial f_S}{\partial T}$) in Eq. (4) can be considered as a pseudo specific heat and an apparent specific heat (c') can be defined, and this equation can be written as:

$$\rho.c' \frac{\partial T}{\partial t} = k\left(\frac{\partial^2 T}{\partial x^2}\right) \tag{5}$$

The introduction of finite difference terms in Eq. (5), gives:

$$\rho c'\left(\frac{T_i^{n+1} - T_i^n}{\Delta t}\right) = k\left(\frac{T_{i-1}^n - 2T_i^n + T_{i+1}^n}{\Delta x^2}\right) \tag{6}$$

where the subscripts indicate the node address on the spatial network and the superscripts represent time. By multiplying Eq. (6) by ($\Delta x.\Delta y.\Delta z$), yields:

$$A_T \Delta x \rho c'\left(\frac{T_i^{n+1} - T_i^n}{\Delta t}\right) = A_T k\left(\frac{T_{i+1}^n + T_{i-1}^n - 2T_i^n}{\Delta x}\right) \tag{7}$$

where $A_T = \Delta y.\Delta z$ [m^2], and y and z are the distances respectively along y-axis and z-axis. By applying an analogy between electrical and thermal circuits, the energy accumulated in a volume element i, is given by:

$$C_{Ti} = A_T.\ \Delta x_i.\rho_i.c_i' = V.\rho_i.c_i' \tag{8}$$

where V is the finite volume element [m^3], and C_{Ti} is the thermal capacitance [J/kg].

The thermal resistance at the heat flux line x can be calculated for each element, and given by:

$$R_{i+1} = \frac{\Delta x_{i+1}}{2k_{i+1}A_T} \tag{9}$$

$$R_{i-1} = \frac{\Delta x_{i-1}}{2k_{i-1}A_T} \tag{10}$$

$$R_i = \frac{\Delta x_i}{2k_i A_T} \tag{11}$$

By introducing Eq. (8) ,(9), (10) and (11) into Eq. (7), yields:

$$C_{Ti}\left(\frac{T_i^{n+1} - T_i^n}{\Delta t}\right) = \left(\frac{T_{i+1}^n - T_i^n}{R_{i+1} + R_i}\right) + \left(\frac{T_{i-1}^n - T_i^n}{R_{i-1} + R_i}\right) \tag{12}$$

or

$$T_i^{n+1} = \left(\frac{\Delta t}{\tau_{Qi}}\right)T_{i+1}^n + \left[1 - \frac{\Delta t}{\tau_{QDi}}\right]T_i^n + \left(\frac{\Delta t}{\tau_{Di}}\right)T_{i-1}^n \tag{13}$$

where:

$$\tau_{Qi} = C_{Ti}(R_{i+1} + R_i) \tag{14}$$

$$\tau_{Di} = C_{Ti}(R_{i-1} + R_i) \tag{15}$$

$$\tau_{QDi} = \frac{\tau_{Qi}.\tau_{Di}}{\tau_{Qi} + \tau_{Di}} \tag{16}$$

Eq. (13) represents the solution of the explicit form of the finite difference method, and will be stable for $\Delta t \le \tau_{QDi}$. A three dimensional version of this solution has been recently applied for cases of complex shaped bodies [Spim, 1997] and a two dimensional version has been applied to continuous casting [Santos, 2000, 2005, 2006].

3. EXPERIMENTAL PROCEDURE AND NUMERICAL SIMULATIONS

The chemical composition and the austenitizing temperatures selected for experimentation, and the employed thermophysical properties are summarized in Table 1.

Table 1. Chemical composition, Jominy test conditions and thermophysical properties.

SAE 1045 - Chemical Composition (wt%) * optical emission spectrometry						
% C 0.45	% Si 0.192	% Mn 0.730	% P 0.0159	% S 0.0366	% Cr 0.0642	% Mo 0.0260
% Ni 0.0703	% Al 0.0022	% Cu 0.146	% Ti 0.00462	% Pb -	% Sn < 0.005	% Fe Balance
Austenitic Temperature (^oC)						
850		900			950	
THERMOPHYSICAL PROPERTIES (20 – 950 ^oC)						
ks (W/m.K) $54 - 3.33x10^{-2} . T$		cs (J/kg.K) $425 + 7.73x10^{-1} . T - 1.69x10^{-3} . T^2 + 2.22x10^{-6} . T^3$			ρs (kg/m^3) 7833	

A numerical expression was used to determine the martensite start temperature (M_S) as a function of composition, given by [ASM Handbook, v. 4]:

$$M_S = 512 - 453.\%C - 16.9.\%Ni + 15.\%Cr - 9.5.\%Mo + 217.(\%C)^2 - 71.5.(\%C - Mn) - 67.9.(\%C - Cr) \tag{23}$$

and the following expressions were used to calculate critical temperatures A1(the temperature at which transformation of austenite to ferrite or to ferrite plus cementita is completed during cooling) and A3 (the temperature at which austenite begins to transform to ferrite during cooling):

$$\mathrm{A1} = 723 - 20.7.\%\mathrm{Mn} - 16.9.\%\mathrm{Ni} + 29.1.\%\mathrm{Si} - 16.9.\%\mathrm{Cr} \tag{24}$$

$$\mathrm{A3} = 910 - 203.\sqrt{\%\mathrm{C}} - 15.2.\%\mathrm{Ni} + 44.7.\%\mathrm{Si} + 104.\%\mathrm{V} + 31.5.\%\mathrm{Mo} \tag{25}$$

A one-dimensional model of the metal/cooling system that predicts the thermal field in a longitudinal section through the system was used to provide a forward problem solution. The application to the model of quench-end test was based on the following key assumptions: (a) one-dimensional heat transfer phenomenon was considered with heat flux admitted along the vertical x-direction; (b) the isothermal moving was assumed to be flat; (c) an overall heat transfer coefficient characterizes the interfacial heat transfer between metal surface and cooling water; (d) the metal temperature is considered equal to the austenitizing temperature; (e) the physical properties were evaluated to taking into account the temperature. A schematic representation of the longitudinal section is shown in Figure 5a.

Experiments in Jominy Test were performed with SAE 1045 steel with austenitizing temperature: 850°C, 900°C and 950°C. Two diametrically opposite flats (0.38 mm - 0.015 inch) deep and parallel to the axis of the bar were ground and the hardness was measured along the flats. The specimens were prepared for hardness testing according specifications of ASTM Standard A 225 and E 18. To ensure reproducibility of results, twos flats were measured for each selection position. The longitudinal section, as indicated in Fig. 5b, was polished and etched to reveal the microstructure. The used reagent was Nital 3%. An optical microscopy and an image processing system were used to acquire images about the microstructures.

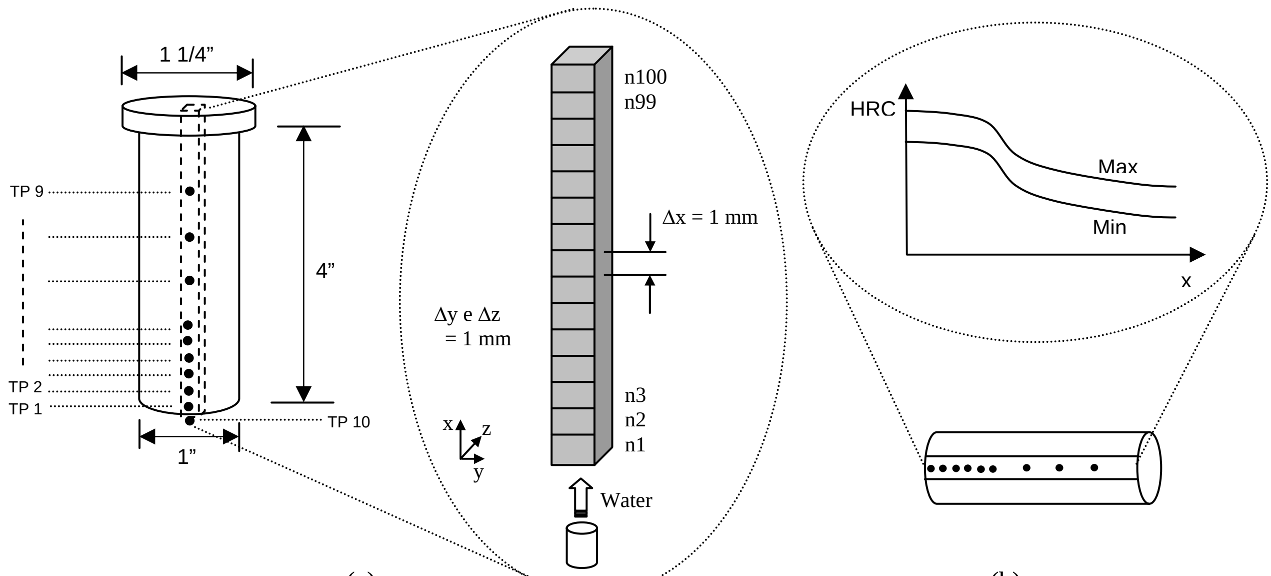

(a) (b)

Figure 5. Schematic representations: (a) longitudinal section of the specimen, (b) hardenability curve.

4. RESULTS AND DISCUSSION

The results of simulated cooling curves in metal have been used to determine the cooling rate as a function of time and position, as indicated in Figure 6.

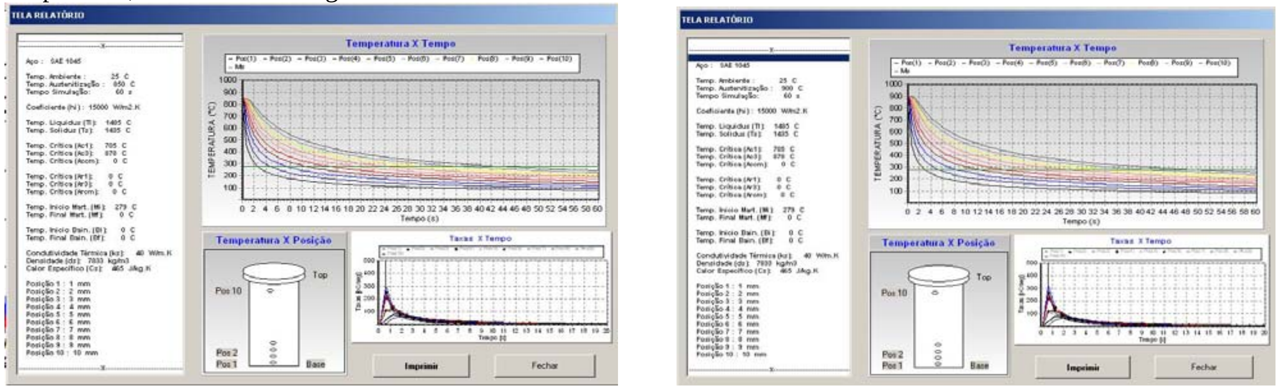

Figure 6. Simulated results: austenitic temperature = 850 °C and 900 °C.

The microstructures in the longitudinal direction reveal the phases, as shown in Fig. 7.

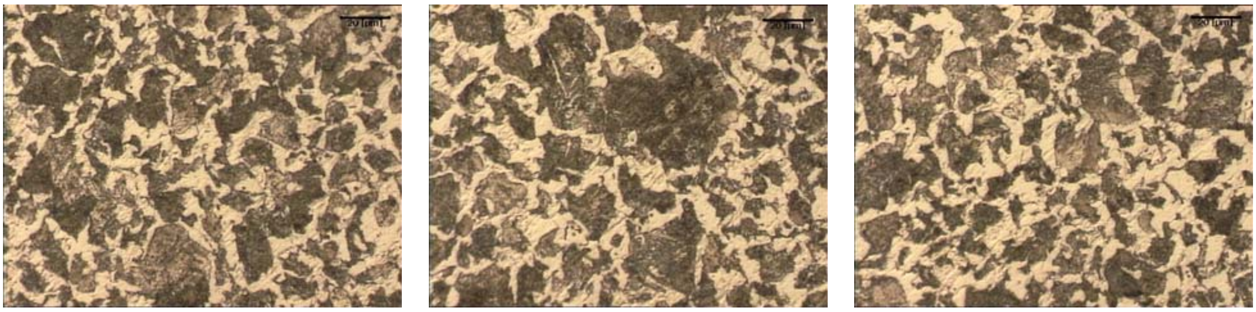

Fig. 7. Microstructure of some positions (longitudinal section) in the specimen (Nital, 500x).

The microstructures in the longitudinal direction reveal the phases, as shown in Fig. 8.

850°C | 900°C | 950°C

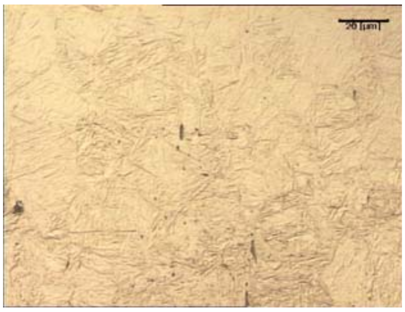
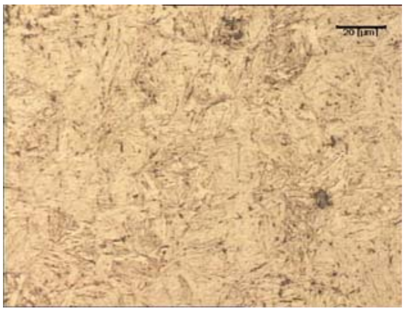


Position 1/16” (1.59 mm) | Position 1/16” (1.59 mm) | Position 1/16” (1.59 mm)

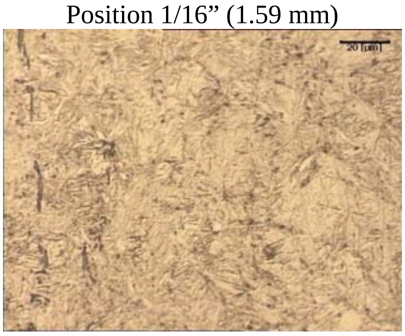
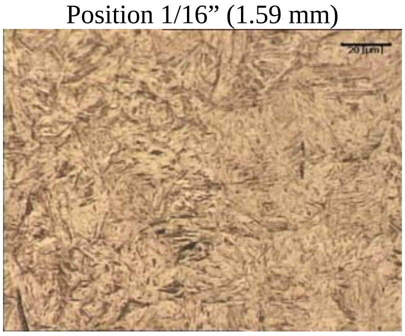
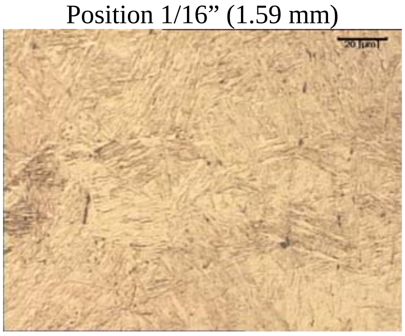

Position 2/16” (3.17 mm) | Position 2/16” (3.17 mm) | Position 2/16” (3.17 mm)

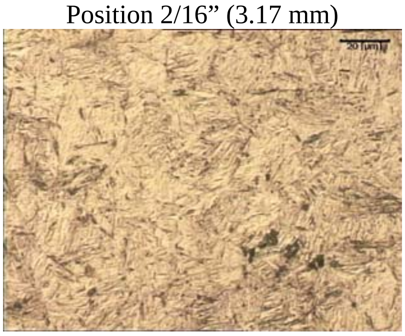
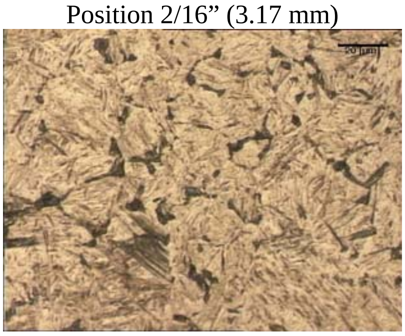
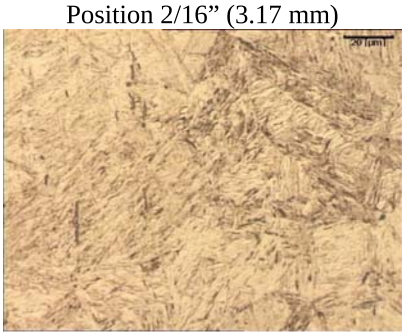

Position 3/16” (4.76 mm) | Position 3/16” (4.76 mm) | Position 3/16” (4.76 mm)

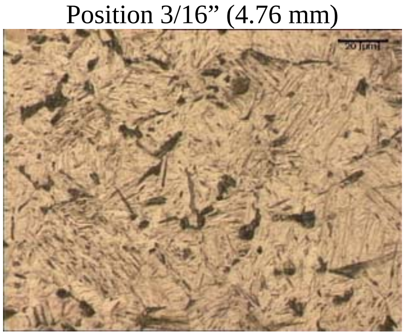
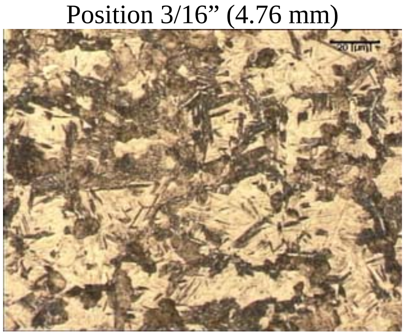
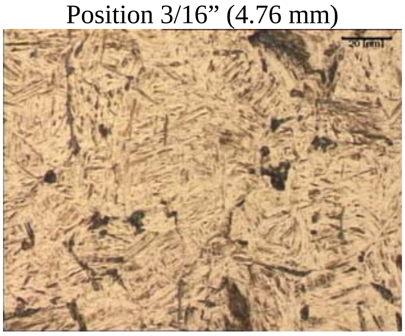

Position 4/16” (6.35 mm) | Position 4/16” (6.35 mm) | Position 4/16” (6.35 mm)

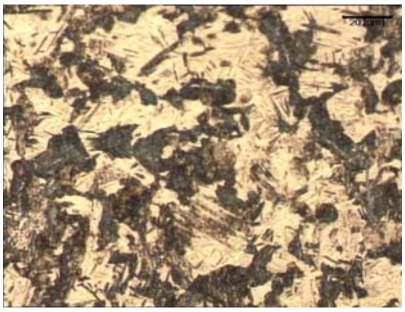
Position 5/16” (7.93 mm)

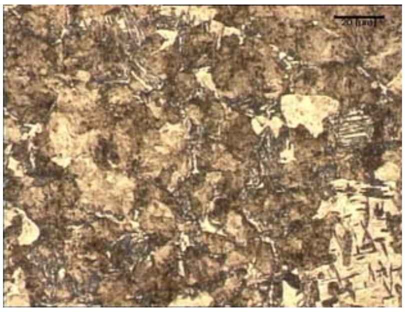
Position 5/16” (7.93 mm)

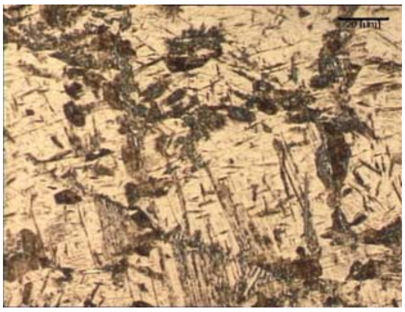
Position 5/16” (7.93 mm)


Position 6/16” (9.52 mm)

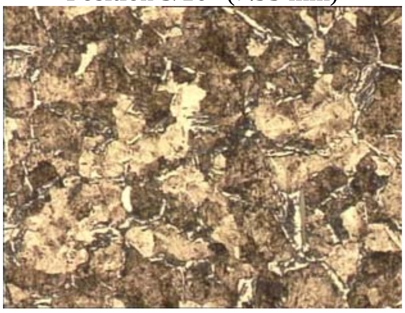
Position 6/16” (9.52 mm)


Position 6/16” (9.52 mm)

Fig. 8. Microstructure of some positions (longitudinal section) in the specimen (Nital, 500x).

As can be observed in Fig. 9, the microstructure of the 950°C shows a high average grain size as compared to 850°C. The hardness measurements were plotted as a function of distance from end quench, as shown in graphic of Fig. 9.

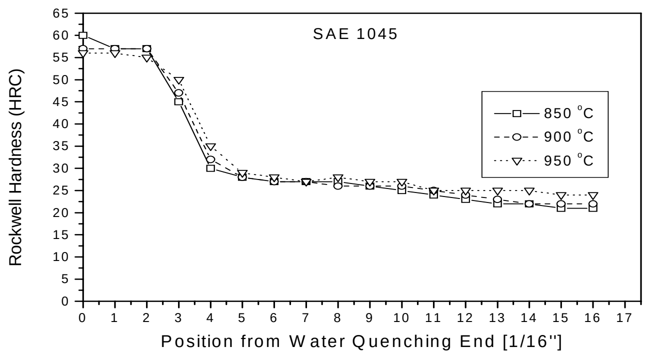

Fig. 9. Hardenability curve for each experiment: (a) 850°C; (b) 900°C; (c) 950°C.

The simulation results about cooling rates were compared with continuous-cooling-transformation, as shown in graphic of Fig. 10. The critical cooling rates are: 825 °C/s (90% Martensite); 113 °C/s (50% Martensite) and 12 °C/s (0% Martensite).

Simulation (a) – Tγ = 850 °C:	Position 1 mm	⇒	Cooling rate > 90% M
	Position 3 mm	⇒	Cooling rate > 85% M
	Position 5 mm	⇒	Cooling rate > 70% M
	Position 7 mm	⇒	Cooling rate > 65% M
	Position 9 mm	⇒	Cooling rate > 60 % M
Simulation (a) – Tγ = 900 °C:	Position 1 mm	⇒	Cooling rate > 90% M
	Position 3 mm	⇒	Cooling rate > 80% M
	Position 5 mm	⇒	Cooling rate > 75% M
	Position 7 mm	⇒	Cooling rate > 65% M
	Position 9 mm	⇒	Cooling rate > 60 % M
Simulation (a) – Tγ = 950 °C:	Position 1 mm	⇒	Cooling rate > 90% M
	Position 3 mm	⇒	Cooling rate > 80% M
	Position 5 mm	⇒	Cooling rate > 80% M
	Position 7 mm	⇒	Cooling rate > 65% M
	Position 9 mm	⇒	Cooling rate > 60 % M

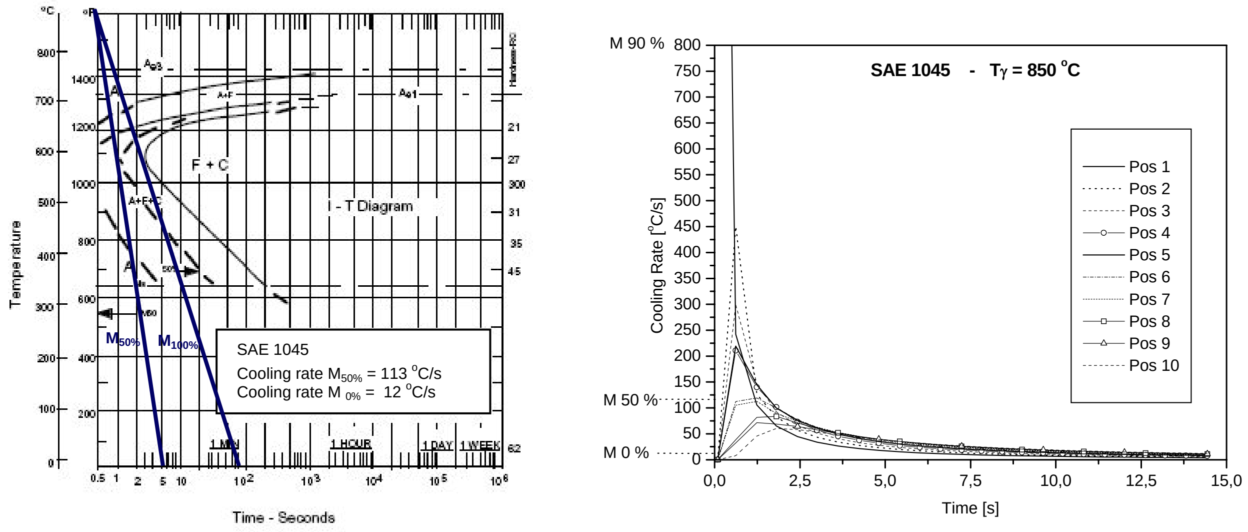

(a)

(b)

Fig. 10. Continuous-cooling-transformation diagram of the SAE 1045 and the estimated cooling rates (a): 850°C.

5. CONCLUSIONS

A mathematical model of steel quenching has been developed to predict the distribution of microstructure and mechanical properties in the Jominy test. The characteristic cooling rate, relevant for structure transformation for structural steels is the relation between time of cooling from austenitic temperature to Ms. The austenite decomposition results were estimated based on cooling rate and Mi. The numerical simulations produce qualitatively results. The microstructural evolution in the SAE 1045 could be easily followed by optical microscopy and hardness. A further interesting line of research is to incorporate thermocouples in the Jominy specimen.

6. ACKNOWLEDGEMENTS

The authors would like to acknowledge support provided by FAPERGS (The Scientific Research Foundation of Rio Grande do Sul), CNPq (The Brazilian Research Council) and COLCIENCIAS (The Colombian Research Council).

7. REFERENCES

ASTM A 255 Standard Test Methods for Determining Hardenability of Steel. ASTM International, 2005.

ASM Handbook v. 4 – Heat Treating. ASM International, 1991.

ASTM Standard E 18 Standard Test Methods for Rockwell Hardness and Rockwell Superficial Hardness of Metallic Materials. ASTM Standards. ASTM, 100 Barr Harbor Drive, West Conshohocken, PA 19428-2959, United States.

CHIAVERINNI, V. Aços e Ferros Fundidos. Associação Brasileira de Metalurgia e Materiais, 7a Edição, 2005.

COSTA E SILVA, A.L.V., Mei, P.R. Aços e Ligas Especiais. Editora Edgard Blucher, 2ª Edição, 2006.

Homberg, D. A Numerical Simulation of the Jominy End-Quench Test. Acta Materialia, v.44, n.11, pp.4375-4385, 1996.

Masson, P.L.; Loulou, T.; Artioukhine, E.; Rogeon, P.; Carron, D.; Quemener, J.J. A numerical study for the estimation of a convection heat transfer coefficient during a metallurgical "Jominy end-quench" test. International Journal of Thermal Sciences, v.41, pp.517–527, 2002.

SONG Y.P.; Liu, G.Q.; Liu, S.X., Liu, J.T., Feng, C.M.. Improved Nonlinear Equation Method for Numerical Prediction of Jominy End-Quench Curve. Journal of the Iron and Steel Research, International, v.14, n.1, pp.37-41, 2007.

SPIM, J.A.; Aplicação da Modelagem Matemática na Definição Integral da Solidificação para Projeto ou Reprogramação de Sistema de Fundição. Tese de Doutorado, UNICAMP/FEM/DEMA, 1996.

SPIM, J.A.; Garcia, A.; An Optimization of the Finite Difference Method for Modeling Solidification of Complex Shaped Domains. Journal of the Brazilian Society of Mechanical Sciences, v.XIX, n.3, pp.392-409, 1997.

SANTOS, C.A.; Garcia, A.; Frick, C.R.F.; Spim, J.A. Evaluation of Heat Transfer Coefficients along the Secondary Cooling Zones in the Continuous Casting of Steel Billets. Inverse Problems in Engineering, United Kingdom, v.14, n.6, pp.687-700, 2006.

SANTOS, C. A. ; Spim, J.A.; Garcia, A. Modeling of Solidification in the Twin-Roll Strip Casting. Journal of Materials Processing Technology, Inglaterra, v.102, pp.33-39, 2000.

INCROPERA, F.P.; Dewitt, D.P. Fundamentals of Heat and Mass Transfer, John Wiley & Sons, 3rd Edition, 1990.